

# VSC-Based DSTATCOM for PQ Improvement: A Deep-Learning Approach

Research Article

Mrutyunjaya Mangaraj<sup>1</sup>, Jogeswara Sabat<sup>1,\*</sup>, Ajit Kumar Barisal<sup>2</sup>, K. Subba Ramaiah<sup>1</sup>, Gudivada Eswara Rao<sup>3</sup>

<sup>1</sup>Department of Electrical and Electronics Engineering, Lendi Institute of Engineering and Technology, Vizianagaram, Andhra Pradesh 535005, India

<sup>2</sup>Department of Electrical Engineering, Odisha University of Technology and Research, Bhubaneswar, Odisha 751029, India

<sup>3</sup>Department of Electrical and Electronics Engineering, Vignan Institute of Technology and Management, Berhampur, Odisha 761008, India

Received: April 17, 2022; Accepted: June 29, 2022

**Abstract:** With the rapid advancement of the technology, deep learning supported voltage source converter (VSC)-based distributed static compensator (DSTATCOM) for power quality (PQ) improvement has attracted significant interest due to its high accuracy. In this paper, six subnets are structured for the proposed deep learning approach (DL-Approach) algorithm by using its own mathematical equations. Three subnets for active and the other three for reactive weight components are used to extract the fundamental component of the load current. These updated weights are utilised for the generation of the reference source currents for VSC. Hysteresis current controllers (HCCs) are employed in each phase in which generated switching signal patterns need to be carried out from both predicted reference source current and actual source current. As a result, the proposed technique achieves better dynamic performance, less computation burden and better estimation speed. Consequently, the results were obtained for different loading conditions using MATLAB/Simulink software. Finally, the feasibility was effective as per the benchmark of IEEE guidelines in response to harmonics curtailment, power factor (p.f) improvement, load balancing and voltage regulation.

**Keywords:** DL-Approach • DSTATCOM • ALMS and PQ

## Abbreviations

DL-Approach, deep-learning approach; DSTATCOM, distributed static compensator; HCC, hysteresis current controller; IGBT, insulated gate bipolar transistor; NN, neural network; PCC, point of common coupling; p.f., power factor; PQ, power quality; THD, total harmonic distortion; VSC, voltage source converter.

## 1. Introduction

With the proliferation of industrial, commercial, residential, irrigation, traction and electric vehicle charging stations, the power quality (PQ) problem is very severe. The PQ issues can be suppressed by different active and passive filtering solutions reported in various published articles (Bayu 2020; Liu et al., 2018, 2022; Pan et al., 2017; Tang et al., 2012). In Liu et al. (2018) and Pan et al. (2017), it is noticed that active filtering has more flexibility and high efficiency compared with passive filtering. In the meantime, PQ analysis is becoming increasingly significant for planning, operation and control of voltage source converter (VSC)-based custom power devices in the distribution system.

In view of this, various advanced and adaptive algorithms have been developed to control the active devices for the PQ improvement. Some of these algorithms are adaptive Neural network (NN) (Mangaraj et al., 2022),

\* Email: jogesh.electrical@gmail.com

hybrid NN (Mangaraj et al., 2017; Panda and Mangaraj, 2017), Leaky LMS (Arya and Singh 2013), adaptive neuro-fuzzy inference system (Badoni et al., 2016), Artificial NN-based discrete-fuzzy logic (Saribulut et al., 2014), LMBP (Levenberg–Marquardt back propagation) Training Based Control Technique (Mangaraj et al., 2020), KHLMS (Kernel Hebbian least mean square) algorithm (Mangaraj et al., 2019), Combined LMS–LMF-(least mean square–least mean fourth) Based Control Algorithm (Srinivas et al., 2016), Hebbian Learning (Siri et al., 2008) and Hebbian/Anti-Hebbian NN (Mangaraj 2021; Pehlevan et al., 2015). NN-based control algorithm has several attributes that make it very suitable for distributed static compensator (DSTATCOM). However, the adaptive controller for DSTATCOM has more computational time for better convergence characteristics. It does not restrict to the unessential weight connection to get a tuned weight which is an additional burden. The appropriate network structure is also a difficult task to accommodate with different step sizes, learning rates, initial weights, updated weights and other associated weights (Arya et al., 2015; Papadopoulos et al., 2016; Qasim et al., 2014).

In this paper, a deep learning approach (DL-Approach) is proposed to overcome the above limitations of these NN techniques. Deep belief networks substitute simple arrangements instead of complex arrangements and eliminate the unessential weights and connection structure (Cai et al., 2019; Zhang et al., 2018). Thus, a deep belief network with the same overall architecture as a corresponding deep NN is defined and trained. Then, its weights are taken and placed into the corresponding deep NN, which is then fine-tuned and put to the application (Li et al., 2022). Hence, it possesses several advantages such as (i) it reduces computational time as it grows linearly in computational structures and connection weights and (ii) these are significantly less vulnerable to the vanishing gradients problem. In practice, the above-mentioned advantages have worked significantly for further advantages for the PQ solution (Liao et al., 2018; Zhang and Mao, 2020). Among them are: (1) Faster response in both steady and dynamic states is obtained through (a) prediction of updated weight and (b) possible inclusion of modified control weights; and (2) Provides flexibility for each leg of VSC independently: (a) better-quality of grid currents is achieved, (b) achievement of compensation currents is performed, (c) switching frequency and reduction of VSC rating are gained and (d) flexibility for switching operation are provided.

The above said literature review has resulted in achieving the following objectives:

- (i) The performance of the DL-Approach control technique for the distribution system has been improved because of inherent merits such as high convergence speed characteristics, stability, reliability, adaptability and high-speed data processing. Also, it minimises the switching and conduction losses.
- (ii) The power rating of VSC is reduced. Some other PQ improvements are also achieved such as power factor (p.f) correction, better voltage regulation, balanced voltage at the point of common coupling (PCC) and source current shaping.
- (iii) Besides the above advantages, the DL-Approach is also competent for the signal attributes such as reliable operation, frequency, p.f and amplitude.

This paper is organised as follows. Section 2 introduces the design and modelling of two level VSC-based DSTATCOM for three phase three wire Distribution System. Section 3 presents the mathematical formulation of ALMS (Adaptive Least Mean Square)/DL-Approach control algorithms. Section 4 shows the simulation results to verify the superiority of DL-Approach DSTATCOM. Finally, the summary of the research work is presented in Section 5.

## 2. Design and Modelling of Two-Level VSC-Based DSTATCOM for 3P3W Distribution System

The structural diagram of the proposed distribution system with ALMS and DL-Approach-based DSTATCOM is shown in Figure 1. It consists of three-phase DSTATCOM, three-phase source and three-phase nonlinear load. The DSTATCOM is regarded as three phase three wire two level VSC. The VSC contains a self-supported capacitor and six insulated gate bipolar transistor (IGBT) switches. Three interfacing impedances ( $Z_{ca}, Z_{cb}, Z_{cc}$ ) are connected in series at the output of VSC to cancel the ripple currents. The compensating currents ( $i_{ca}, i_{cb}, i_{cc}$ ) are injected to cancel the reactive power components and harmonics of the load currents so that source currents ( $i_{sa}, i_{sb}, i_{sc}$ ) harmonics are reduced in the distribution system. A model of a 3-phase voltage inverter with an L-type

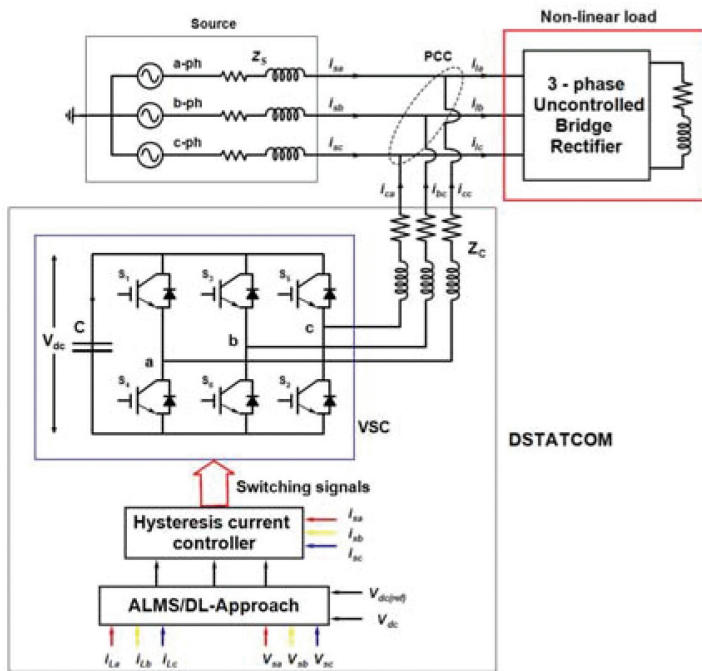


Fig. 1. Block diagram representation of power distribution system.

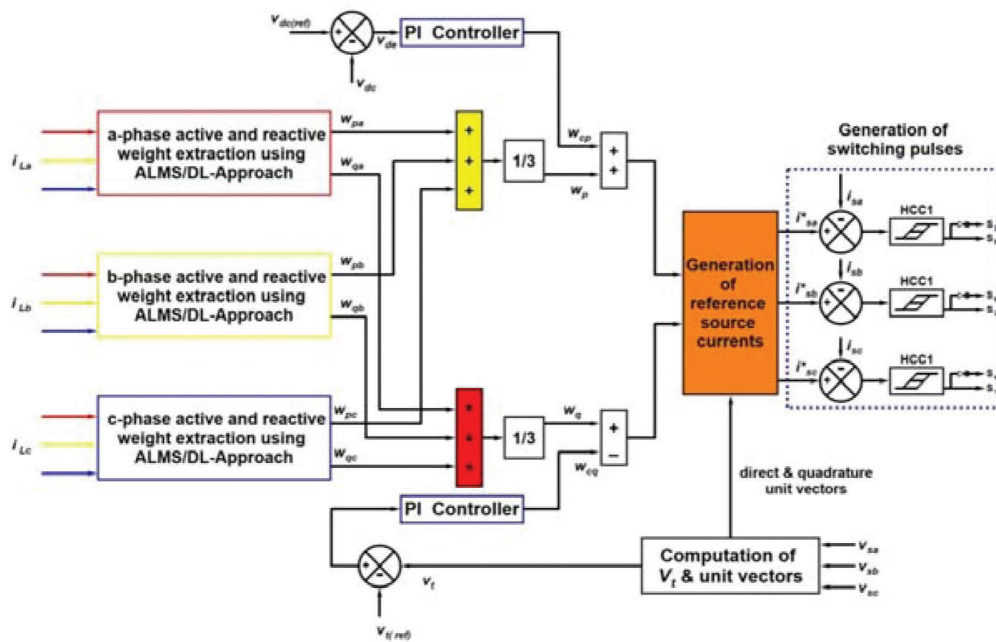


Fig. 2. ALMS/DL-Approach control technique principle. DL-Approach, deep-learning approach.

output filter was adopted rather than LC (inductor and capacitor) or LCL (inductor, capacitor and inductor) filters (Figure 1). In Figure 1, voltage source inverter-based DSTATCOM topology is considered which consists of self-supported capacitor, voltage source inverter and interfacing inductor. This interfacing inductor is used to smoothen the ripple in the inverter output current and provides the reactive power as per the load variation (Singh et al., 2014). The complete procedure for the switching signal generation of DSTATCOM is shown in Figure 2.

### 3. Mathematical Formulation of Control Algorithm

The circuit explanation of two control algorithms is presented separately as follows.

#### 3.1. ALMS control technique

In this section, the ALMS control technique used the proper mathematical investigation with different behaviours associated with the rate of learning and step size, unit input weights and bias. The complete procedure for the switching signal generation is shown in Figure 2.

The main purpose is to provide an individual phase tuned weight corresponding to the fundamental frequency real component of the load current. The learning mechanism is expressed as per the following iteration:

The extraction of weighting values of fundamental active component of load current ( $w_{pa}, w_{pb}, w_{pc}$ ) can be calculated as

$$w_{pa}(n) = \alpha\gamma \{i_{la}(n) - w_{pa}(n-1)u_{pa}(n)\}u_{pa}(n) + w_{pa}(n-1) \quad (1)$$

$$w_{pb}(n) = \alpha\gamma \{i_{lb}(n) - w_{pb}(n-1)u_{pb}(n)\}u_{pb}(n) + w_{pb}(n-1) \quad (2)$$

$$w_{pc}(n) = \alpha\gamma \{i_{lc}(n) - w_{pc}(n-1)u_{pc}(n)\}u_{pc}(n) + w_{pc}(n-1) \quad (3)$$

Similarly, the extraction of weighting values of fundamental reactive component of load current ( $w_{qa}, w_{qb}, w_{qc}$ ) can be calculated as

$$w_{qa}(n) = \alpha\gamma \{i_{la}(n) - w_{qa}(n-1)u_{qa}(n)\}u_{qa}(n) + w_{qa}(n-1) \quad (4)$$

$$w_{qb}(n) = \alpha\gamma \{i_{lb}(n) - w_{qb}(n-1)u_{qb}(n)\}u_{qb}(n) + w_{qb}(n-1) \quad (5)$$

$$w_{qc}(n) = \alpha\gamma \{i_{lc}(n) - w_{qc}(n-1)u_{qc}(n)\}u_{qc}(n) + w_{qc}(n-1) \quad (6)$$

#### 3.2. DL-Approach technique

The DL-Approach is a deep multilayer perceptron (MLP) with input  $h^0$  and L computational layers  $h^i$  ( $i = 1, 2, \dots, L$ ). Each layer  $h^i$  is a Restricted Boltzmann Machine (RBM)  $RBM^i$ , a generative graphical model that encodes the probability density function (PDF) of its input layer  $h^{i-1}$  into its latent feature vector  $h^i$ . At each  $RBM^i$  ( $i = 1, 2, \dots, L$ ), the conditional PDF of the j-th neurons in the visible layer  $h^{i-1}$  and hidden layer  $h^i$  are computed by:

$$P(h_{ja}^i = 1 | h_{ja}^{i-1}) = \sigma \sum_k W_{kj}^i h_k^{i-1} u_{pa}(n) (I_{la}(n) - w_{pa}(n-1) + b_j^i w_{pa}(n-1)) \quad (7)$$

$$P(h_{ja}^i = 1 | h_{ja}^{i-1}) = \sigma \sum_k W_{kj}^i h_k^{i-1} u_{pa}(n) (I_{la}(n) - w_{pa}(n-1) + b_j^i w_{pa}(n-1)) \quad (8)$$

$$P(h_{ja}^i = 1 | h_{ja}^{i-1}) = \sigma \sum_k W_{kj}^i h_k^{i-1} u_{pa}(n) (I_{la}(n) - w_{pa}(n-1) + b_j^i w_{pa}(n-1)) \quad (9)$$

$$P(h_{ja}^i = 1 | h_{ja}^{i-1}) = \sigma \sum_k W_{kj}^i h_k^{i-1} u_{pa}(n) (I_{la}(n) - w_{pa}(n-1) + b_j^i w_{pa}(n-1)) \quad (10)$$

$$P(h_{ja}^i = 1 | h_{ja}^{i-1}) = \sigma \sum_k W_{kj}^i h_k^{i-1} u_{pa}(n) (I_{la}(n) - w_{pa}(n-1) + b_j^i w_{pa}(n-1)) \quad (11)$$

$$P(h_{ja}^i = 1 | h_{ja}^{i-1}) = \sigma \sum_k W_{kj}^i h_k^{i-1} u_{pa}(n) (I_{la}(n) - w_{pa}(n-1) + b_j^i w_{pa}(n-1)) \quad (12)$$

where  $w_{pa}, w_{pb}, w_{pc}$  = weighting values of fundamental reactive component of load current.

$$w_a = \frac{w_{pa} + w_{pb} + w_{pc}}{3} \quad (13)$$

where  $w_a$  = mean values of weighting values.

$$w_r = \frac{w_{qa} + w_{qb} + w_{qc}}{3} \quad (14)$$

$$u_{pa} = \frac{v_{sa}}{v_t}, u_{pb} = \frac{v_{sb}}{v_t}, u_{pc} = \frac{v_{sc}}{v_t} \quad (15)$$

where  $u_{pa}, u_{pb}, u_{pc}$  = in-phase unit voltage templates.

The quadrature unit voltage templates ( $u_{qa}, u_{qb}, u_{qc}$ ) are related to phase voltages, which are expressed as follows:

$$u_{qa} = \frac{u_{pb} + u_{pc}}{\sqrt{3}}, u_{qb} = \frac{3u_{pa} + u_{pb} - u_{pc}}{2\sqrt{3}}, u_{qc} = \frac{-3u_{pa} + u_{pb} - u_{pc}}{2\sqrt{3}} \quad (16)$$

Further,  $v_t$  can be expressed as

$$v_t = \sqrt{\frac{2(v_{sa}^2 + v_{sb}^2 + v_{sc}^2)}{3}} \quad (17)$$

$$v_{de} = v_{dc(ref)} - v_{dc} \quad (18)$$

where  $v_{de}$  error in dc voltage.

$$w_{cp} = k_{pa}v_{de} + k_{ia} \int v_{de} dt \quad (19)$$

$$w_{sp} = w_a + w_{cp} \quad (20)$$

$$v_{te} = v_{t(ref)} - v_t \quad (21)$$

where  $v_t$  = PCC voltage and  $v_{t(ref)}$  = reference PCC voltage.

$$w_{cq} = k_{pr}v_{te} + k_{ir} \int v_{te} dt \quad (22)$$

The difference between the output of PI (proportional integral) controller and the average magnitude of reactive component of load currents is the total reactive components of the reference source current, which can be expressed as:

$$w_{sq} = w_r - w_{cq} \quad (23)$$

$$i_{aa} = w_{sp}u_{pa}, i_{ab} = w_{sp}u_{pb}, i_{ac} = w_{sp}u_{pc} \quad (24)$$

Similarly, the three-phase instantaneous reference source reactive component is estimated by multiplying the quadrature unit voltage template and reactive current component, and these are obtained as

$$i_{ra} = w_{sq}u_{qa}, i_{rb} = w_{sq}u_{qb}, i_{rc} = w_{sq}u_{qc} \quad (25)$$

The summation of active and reactive components of current are called reference source currents and these are obtained as

$$i_{sa}^* = i_{aa} + i_{ra}, i_{sb}^* = i_{ab} + i_{rb}, i_{sc}^* = i_{ac} + i_{rc} \quad (26)$$

## 4. Simulation Results

To validate the superiority of the DL-Approach, the proposed distribution system is designed and simulated using the Sim power system toolbox of MATLAB/Simulink. In practice, the connected load is time-varying (3-phase diode full-bridge rectifier load containing  $R_1 = 10\Omega$  and  $L_1 = 20\text{mH}$ ). Shunt compensation comparison of ALMS and DL-Approach are presented in Table 1. The utilised simulation parameters are given in Table 2. The total harmonic distortion (THD) of the supply current amid under time-varying load conditions is examined.

To illustrate the feasibility, the proposed approach is adopted for PQ improvement for the different case studies. The numerical and simulation performances are evaluated and compared with the ALMS and DL-Approach algorithm.

These case studies are described in the following subsequent section:

- 4.1: ALMS algorithm under time in varying loading
- 4.2: ALMS algorithm under time-varying loading
- 4.3: DL-Approach algorithm under time in varying loading
- 4.4: DL-Approach algorithm under time-varying loading

### 4.1. ALMS algorithm under time in varying loading

Figure 3(a) represents the simulation waveform obtained under time in varying loading, from bottom to top shows the inverter DC-link voltage ( $v_{dc}$ ), DSTATCOM compensating current ( $i_{ca}, i_{cb}, i_{cc}$ ), distribution system supply current ( $i_{sa}, i_{sb}, i_{sc}$ ), system load current ( $i_{la}, i_{lb}, i_{lc}$ ) and system supply voltage ( $v_{sa}, v_{sb}, v_{sc}$ ).

Figure 3(b) shows the phase angle between the phase-a supply voltage and current, it indicates the source side p.f 0.96 and load side p.f 0.87. After compensation, the source side THD% reduced to 4.62%, the inverter DC-link

**Table 1.** Compensation comparison of ALMS and DL-Approach for performance

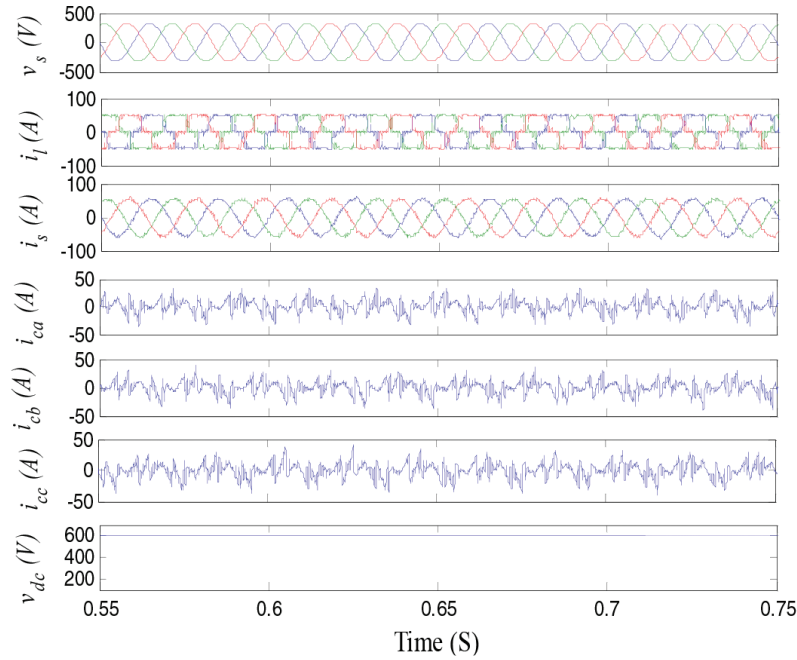
Algorithm	Source current		p.f		$v_{dc}$		Rating of VSC	
	a	b	a	b	a	b	a	b
ALMS	55.88A, 4.62%	50.58A, 4.91%	0.96	0.897	600V	670V	9.288kVA	10.37 kVA
DL-Approach	55.20A, 3.62%	50.68A, 3.81%	0.98	0.94	520V	570V	8.100 kVA	8.92 kVA

DL-Approach, deep-learning approach; p.f, power factor; VSC, voltage source converter.

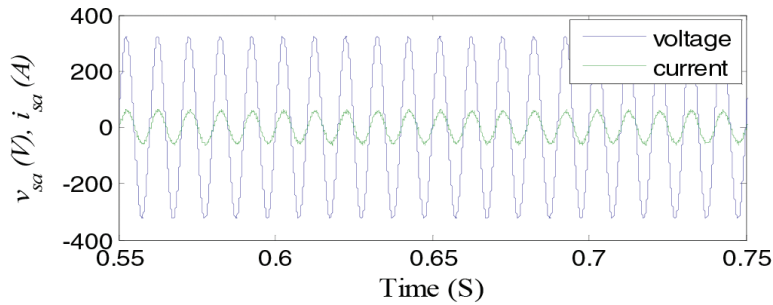
**Table 2.** Simulation parameter design for ALMS/DL-Approach DSTATCOM

Distribution system	Load parameter	Controller parameter	Compensator
$R_s = 0.04\Omega$ $f_s = 50\text{ Hz}$ $L_s = 2\text{ mH}$ (AC main) $v_s = 230\text{ V}$	Nonlinear load: $L_1 = 20\text{ mH}$ $R_1 = 10\Omega$	$v_{i(ref)} = 325\text{ V}$ $\alpha = 0.4$ $v_{dc(ref)} = 600\text{ V}$ $\gamma = 0.2$	$k_{pa} = 0.7$ $k_{pr} = 0.5$ $k_{ia} = 0.1$ $k_{vr} = 0.02$ $C_{dc} = 2.000\mu\text{F}$ $R_c = 0.25\Omega$ $L_c = 1.5\text{ mH}$ Switching frequency= 15kHz IGBT dead Time=2 $\mu\text{s}$ Interfacing inductor value=5mH

DL-Approach, deep-learning approach; DSTATCOM, Distributed Static Compensator; IGBT, Insulated gate bipolar transistor.



(a)



(b)

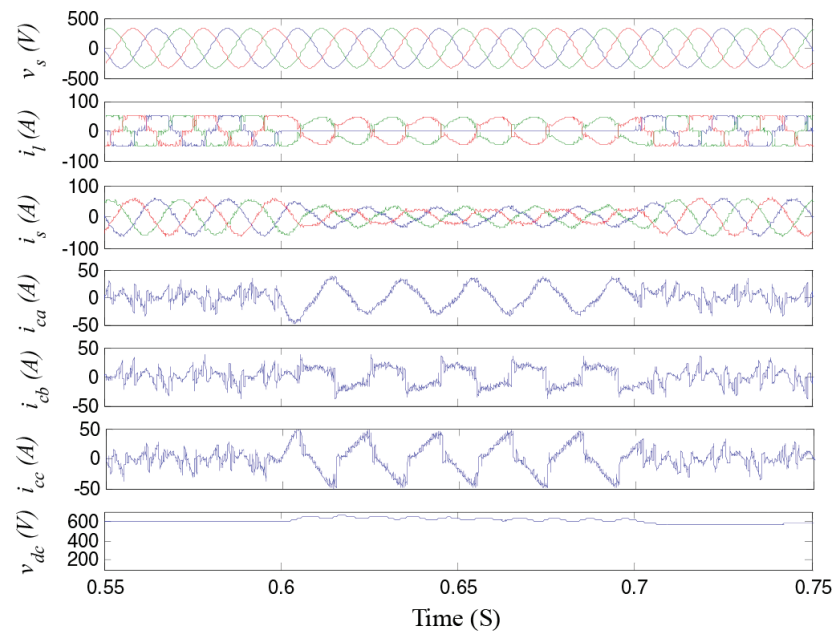
**Fig. 3.** Simulation performance of ALMS algorithm-based DSTATCOM. (a) under time in varying load and (b) for measurement of a-phase input power factor (p.f) due to uniform loading. DSTATCOM, distributed static compensator.

voltage stable at 600 V and the distribution system PCC balance voltage maintained under time in varying loading at the reference value 318 V.

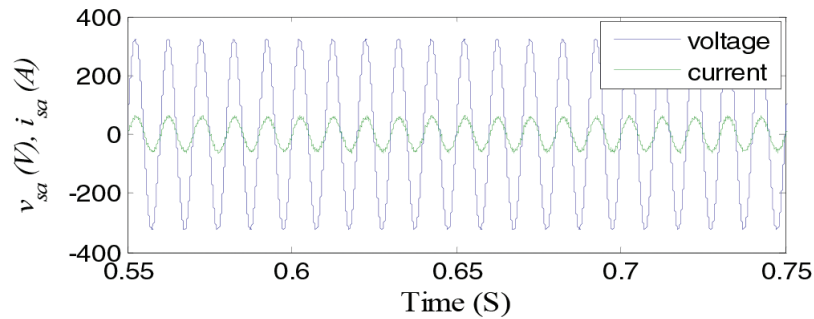
#### 4.2. ALMS algorithm under time-varying loading

To emphasise the better performance of ALMS control technique, Figure 4(a) represents the simulation waveform obtained under time-varying loading, from bottom to top shows the inverter DC-link voltage ( $v_{dc}$ ), DSTATCOM compensating current ( $i_{ca}, i_{cb}, i_{cc}$ ), distribution system supply current ( $i_{sa}, i_{sb}, i_{sc}$ ), system load current ( $i_{la}, i_{lb}, i_{lc}$ ) and system supply voltage ( $v_{sa}, v_{sb}, v_{sc}$ ). Figure 4(b) shows the phase angle between the phase-a supply voltage and current, it indicates the source side p.f 0.897 and load side p.f 0.86. After compensation, the source side THD% reduced 4.91%, the inverter DC-link voltage stable at 670 V and the distribution system PCC balance voltage maintained under time-varying loading at the reference value 317 V.





(a)



(b)

**Fig. 4.** Simulation performance of ALMS algorithm-based DSTATCOM. (a) under time-varying load and (b) for measurement of a-phase input p.f. due to uniform loading. DSTATCOM, distributed static compensator.

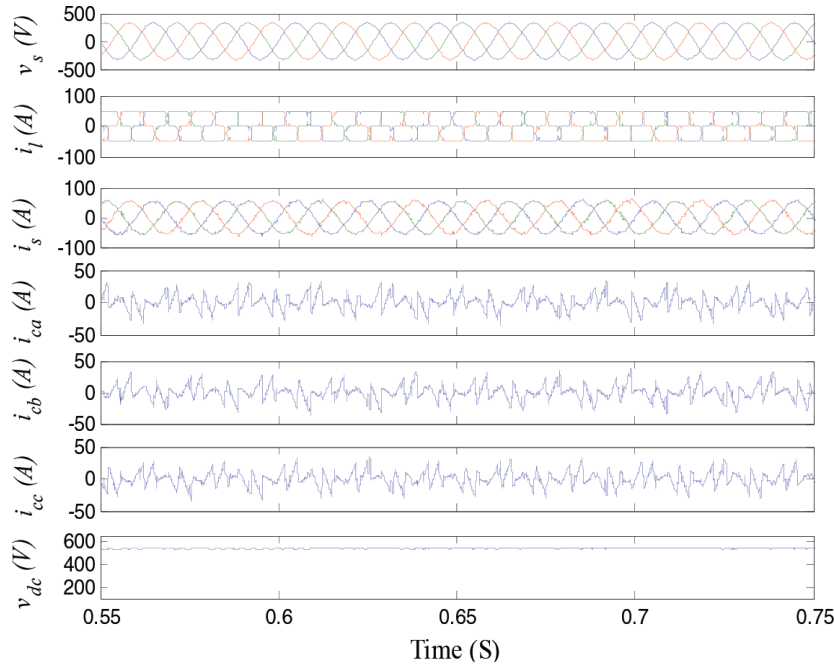
### 4.3. DL-Approach algorithm under time in varying loading

Figure 5(a) represents the simulation waveform obtained under time in varying loading, from bottom to top shows the inverter DC-link voltage ( $v_{dc}$ ), DSTATCOM compensating current ( $i_{ca}, i_{cb}, i_{cc}$ ), distribution system supply current ( $i_{sa}, i_{sb}, i_{sc}$ ), system load current ( $i_{la}, i_{lb}, i_{lc}$ ) and system supply voltage ( $v_{sa}, v_{sb}, v_{sc}$ ). Figure 5(b) shows the phase angle between the phase-a supply voltage and current, it indicates the source side p.f 0.98 and load side p.f 0.87. After compensation, the source side THD% reduced to 3.62%, the inverter DC-link voltage stable at 520 V and the distribution system PCC balance voltage maintained under time in varying loading at the reference value 318V.

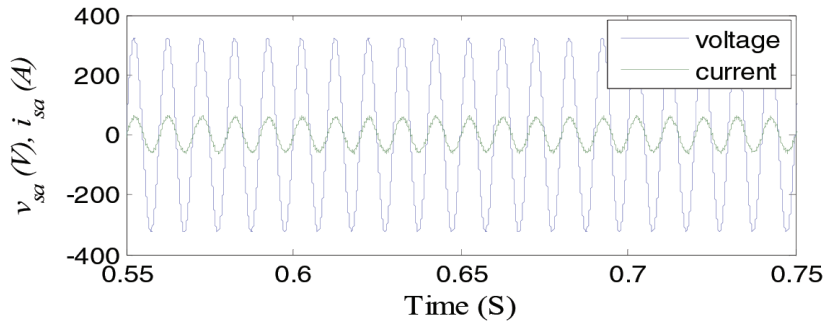
### 4.4. DL-Approach algorithm under time-varying loading

To emphasise the better performance of DL-Approach control technique, Figure 6(a) represents the simulation waveform obtained under time-varying loading, from bottom to top shows the inverter DC-link voltage ( $v_{dc}$ ),





(a)



(b)

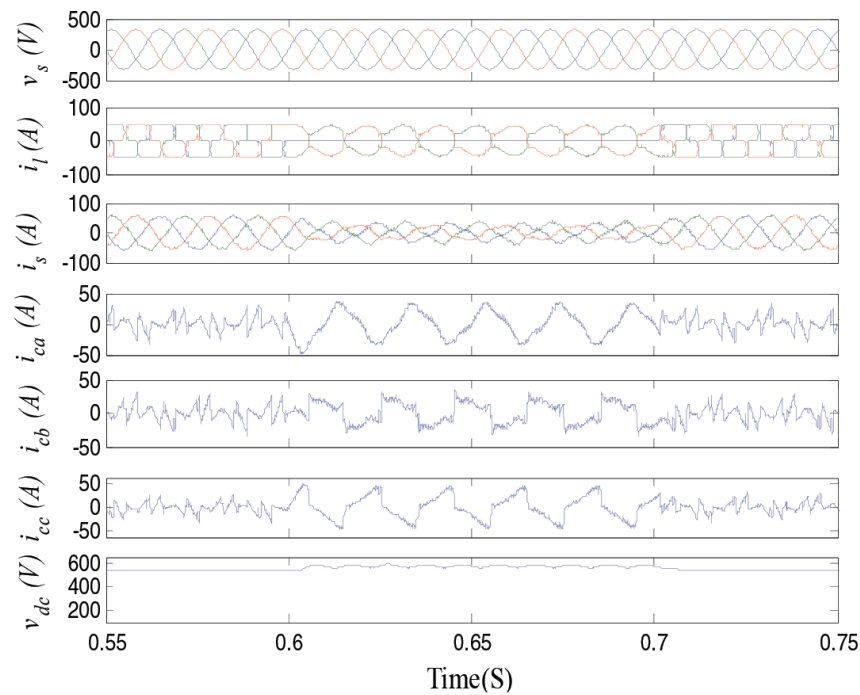
**Fig. 5.** Simulation performance of DL-Approach-based DSTATCOM. (a) under time in varying load and (b) for measurement of a-phase input p.f due to uniform loading. DL-Approach, deep-learning approach; DSTATCOM, distributed static compensator.

DSTATCOM compensating current ( $i_{ca}, i_{cb}, i_{cc}$ ), distribution system supply current ( $i_{sa}, i_{sb}, i_{sc}$ ), system load current ( $i_{la}, i_{lb}, i_{lc}$ ) and system supply voltage ( $v_{sa}, v_{sb}, v_{sc}$ ). Figure 6(b) shows the phase angle between the phase-a supply voltage and current, it indicates the source side p.f 0.94 and load side p.f 0.87. After compensation, the source side THD% reduced to 3.81%, the inverter DC-link voltage stable at 570V and the distribution system PCC balance voltage maintained under time-varying loading at the reference value 317V.

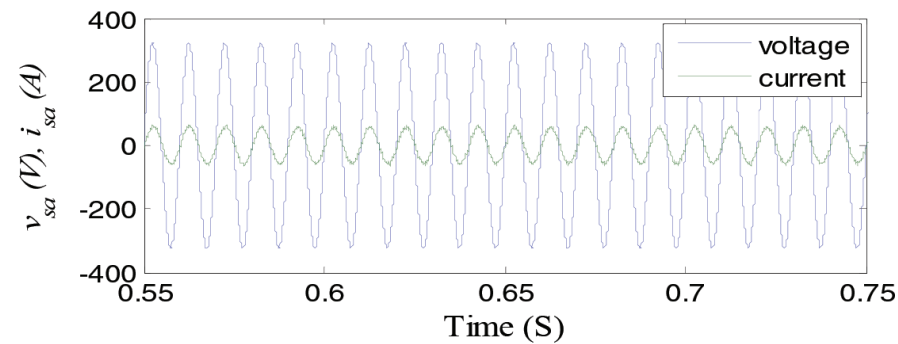
All the above performances are also discussed regarding the different indices based on the capability of the control algorithm, satisfying the grid standards.

#### 4.5. DC-link voltage analysis using ALMS/DL-Approach techniques

In this section, the detailed comparative analysis of  $v_{dc}$  is presented in Figure 7(a) and 7(b). The observation is summarised below:



(a)



(b)

**Fig. 6.** Simulation performance of DL-Approach algorithm-based DSTATCOM. (a) under time in varying load and (b) for measurement of a-phase input p.f due to uniform loading. DL-Approach, deep-learning approach; DSTATCOM, distributed static compensator.

ALMS technique achieved stable 600 V DC-link voltage under time in varying loading and 670 V under time-varying loading.

DL-Approach technique achieved stable 520 V DC-link voltage under time in varying loading and 570 V under time-varying loading.

#### 4.6. Compensation analysis

The Compensation analysis using proposed controller is compared below:

- The THD of source current is 3.62% under time in varying loading conditions and 3.81% under time-varying loading conditions using DL-Approach control technique. It indicates that the value of the DC-link voltage dropped around 22% using the DL-Approach algorithm as compared to the ALMS algorithm.

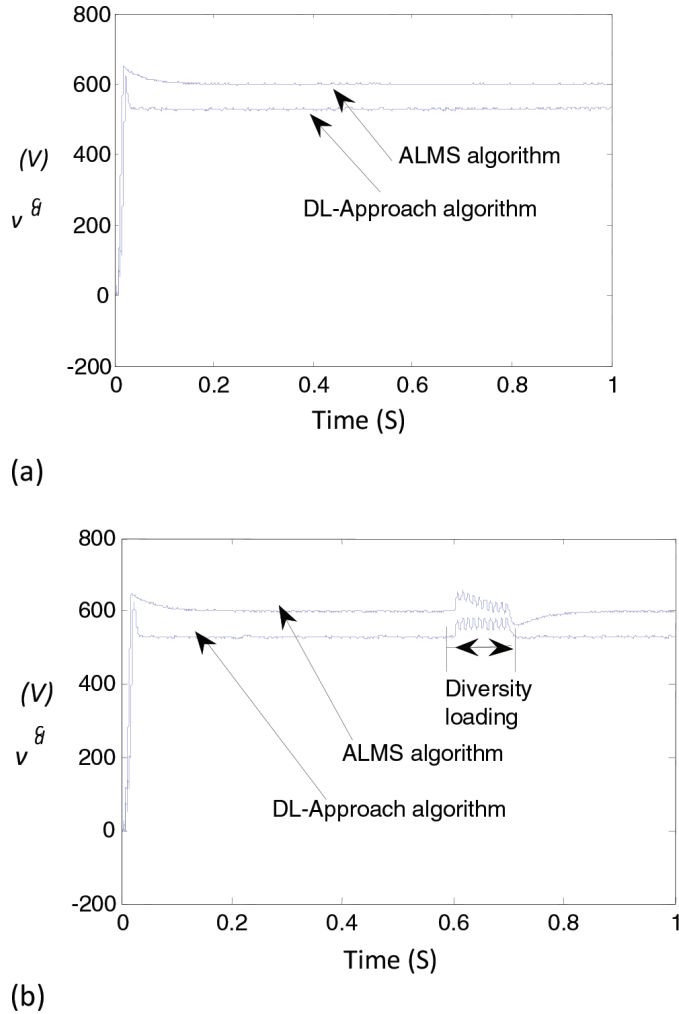


**Fig. 7.** DC-link voltage using both ALMS and DL-Approach technique under (a) time in varying loading and (b) time-varying loading. DL-Approach, deep-learning approach.

- The additional advantages are reduced capacitor stress, minimised DSTATCOM size and a lesser amount of stored energy obtained from the proposed algorithm, and they are also presented in Table 1.
- Therefore, the power rating of the compensator is minimised to nearly 83% (from 9.28 kVA to 8.100 kVA) under time in varying loading whereas 83.09% (from 10.372 kVA to 8.619 kVA) under time-varying loading.

The performance of DL-Approach-based DSTATCOM shows that displacement p.f is improved even after the load change. After compensation, the three-phase source currents THDs are reduced to 3.62% (balanced loading) and 3.81% (unbalanced loading). The average p.f after compensation is 0.98. To achieve better voltage regulation at the DC side, the actual and ref DC link voltages are considered; and to achieve better voltage regulation at the AC side, the PCC and reference AC voltages are considered. The DC link voltage is reduced by DL-Approach, hence the switching stress and filter sizes are reduced compared to ALMS. As the reliability, robustness and tuning of DL-Approach are better, it produces better stability as compared to ALMS.

The THD profile of both ALMS and DL-Approach-based DSTATCOM is shown in Figure 8. The comparative analysis of ALMS and DL-Approach under time in varying and time-varying loading conditions is presented in Table 1.

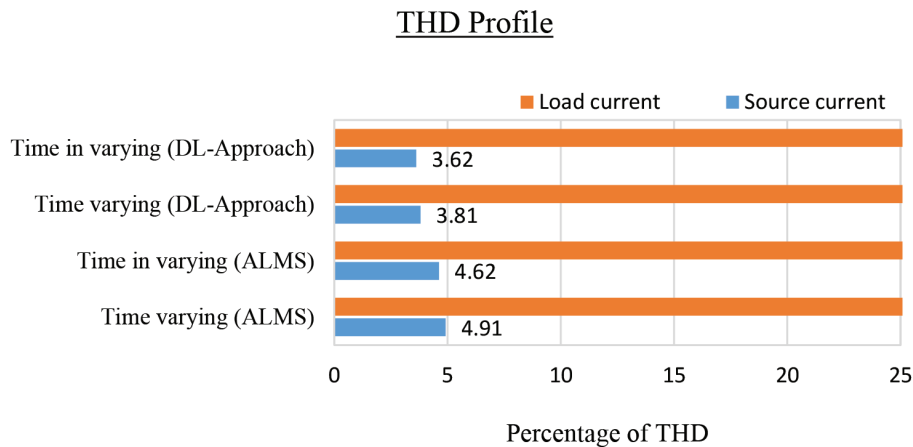


**Fig. 8.** Source and load current THD. THD, total harmonic distortion.

## 5. Conclusion

This study has elaborated two different adaptive control strategies embedded in DSTATCOM for bridging the gap between the NN towards PQ improvement. The proposed DL-Approach control technique showed a valid and flexible structure to accommodate different weighting factors associated with learning mechanisms. Also, it enables corresponding well changes in the VSC configurations for different loading conditions. Numerical results are analysed as per IEEE-514-2017 and IEC (International Electrotechnical Commission)- 61000-1 for PQ, which are presented below:

- After compensation, the source side p.f improvement is achieved.
- Balance voltage is maintained at the PCC of the distribution system.
- DC-link voltage is reduced which further minimised the power rating of DSTATCOM.

## References

- Arya, S. R. and Singh, B. (2013). Performance of DSTATCOM using leaky LMS control algorithm. *IEEE Journal of Emerging and Selected Topics in Power Electronics*, 1(2), pp. 104–113.
- Arya, S. R., Niwas, R., Bhalla, K. K., Singh, B., Chandra, A. and Al-Haddad, K. (2015). Power quality improvement in isolated distributed power generating system using DSTATCOM. *IEEE Transactions on Industry Applications*, 51(6), pp. 4766–4774.
- Badoni, M., Singh, A. and Singh, B. (2016). Adaptive neurofuzzy inference system least-mean-square-based control algorithm for DSTATCOM. *IEEE Transactions on Industrial Informatics*, 12(2), 483–492.
- Bayu, A. (2020). Power quality enhancement using DSTATCOM in industry plants. *Power Electronics and Drives*, 5(1), pp. 157–175. doi:10.2478/pead-2020-0012.
- Cai, K., Cao, W., Aarniovuori, L., Pang, H., Lin, Y. and Li, G. (2019). Classification of power quality disturbances using Wigner-Ville distribution and deep convolutional neural networks. *IEEE Access*, 7, pp. 119099–119109. doi: 10.1109/ACCESS.2019.2937193.
- Li, Y., Li, J. and Wang, Y. (2022). Privacy-preserving spatiotemporal scenario generation of renewable energies: A federated deep generative learning approach. *IEEE Transactions on Industrial Informatics*, 18(4), pp. 2310–2320.
- Liao, H., Milanović, J. V., Rodrigues, M. and Shenfield, A. (2018). Voltage sag estimation in sparsely monitored power systems based on deep learning and system area mapping. *IEEE Transactions on Power Delivery*, 33(6), pp. 3162–3172. doi: 10.1109/TPWRD.2018.2865906.
- Liu, B., Wei, Q., Zou, C. and Duan, S. (2018). Stability analysis of LCL-type grid-connected inverter

- under single-loop inverter-side current control with capacitor voltage feedforward. *IEEE Transactions on Industrial Informatics*, 14(2), pp. 691–702.
- Liu, Y., Zhang, W., Sun, Y., Su, M., Xu, G. and Dan, H. (2022). Review and comparison of control strategies in active power decoupling. *IEEE Transactions on Power Electronics*, 36(12), pp. 14436–14455. doi: 10.1109/TPEL.2021.3087170.
- Mangaraj, M. (2021). Operation of Hebbian least mean square controlled distributed static compensator. *IET Generation, Transmission & Distribution*, 15(3), pp. 1939–1948. doi: 10.1049/gtd2.12146.
- Mangaraj, M. and Panda, A. K. (2017). Performance analysis of DSTATCOM employing various control algorithms. *IET Generation, Transmission and Distribution*, 11(10), pp. 2643–2653.
- Mangaraj, M. and Panda, A. K. (2019). Modelling and simulation of KHLMS algorithm-based DSTATCOM. *IET Power Electronics*, 12(9), pp. 2304–2311.
- Mangaraj, M., Panda, A. K., Penthia, T. and Dash, A. R. (2020). An adaptive LMBP training based control technique for DSTATCOM. *IET Generation, Transmission and Distribution*, 14(3), pp. 516–524.
- Mangaraj, M., Sabat, J., Barisal, A.K., Patra, A.K. and Chahattaray, A.K. (2022). Performance evaluation of BB-QZSI based DSTATCOM under dynamic load condition. *Power Electronics and Drives*, 7(1), pp. 43–55.
- Pan, D., Ruan, X., Wang, X., Yu, H. and Xing, Z. (2017). Analysis and design of current control schemes for LCL-type grid-connected inverter based on a general mathematical model. *IEEE Transactions on Power Electronics*, 32(6), pp. 4395–4410.
- Panda, A. K. and Mangaraj, M. (2017). DSTATCOM employing hybrid neural network control technique for power quality improvement. *IET Power Electronics*, 10(4), pp. 480–489.
- Papadopoulos, S., Rashed, M., Klumpner, C. and Wheeler, P. (2016). Investigations in the modeling and control of a medium-voltage hybrid inverter system that uses a low-voltage/low-power rated auxiliary current source inverter. *Journal of Emerging and Selected Topics in Power Electronics*, 4(1), pp. 126–140.
- Pehlevan, C., Hu, T. and Chklovskii, D. B. (2015). A Hebbian/anti-Hebbian neural network for linear subspace learning: A derivation from multidimensional scaling of streaming data. *International Journal of Neural Computation*, 27(7), pp. 1461–1495.
- Qasim, M., Kanjiya, P. and Khadkikar, V. (2014). Optimal current harmonic extractor based on unified ADALINEs for shunt active power filters. *IEEE Transactions on Power Electronics*, 29(12), pp. 6383–6393.
- Saribulut, L., Teke, A. and Tümay, M. (2014). Artificial neural network-based discrete-fuzzy logic controlled active power filter. *IET Power Electronics*, 7(6), pp. 1536–1546.
- Singh, B., Jayaprakash, P., Kothari, D. P., Chandra, A. and Haddad, K. A. (2014). Comprehensive study of DSTATCOM configurations. *IEEE Transactions on Industrial Informatics*, 10(2), pp. 854–870.
- Siri, B., Berry, H., Cessac, B., Delord, B. and Quoy, M. (2008). A Mathematical analysis of the effects of Hebbian learning rules on the dynamics and structure of discrete-time random recurrent neural networks. *International Journal of Neural Computation*, 20(12), pp. 2937–2966.
- Srinivas, M., Hussain, I. and Singh, B. (2016). Combined LMS–LMF-based control algorithm of DSTATCOM for power quality enhancement in distribution system. *IEEE Transactions on Industrial Electronics*, 63(7), pp. 4160–4168.
- Tang, Y., Loh, P. C., Wang, P., Choo, F. H., Gao, F. and Blaabjerg, F. (2012). Generalized design of high performance shunt active power filter with output LCL filter. *IEEE Transactions on Industrial Electronics*, 59(3), pp. 1443–1452.
- Zhang, D., Han, X. and Deng, C. (2018). Review on the research and practice of deep learning and reinforcement learning in smart grids. *CSEE Journal of Power Energy Systems*, 4(3), pp. 362–370.
- Zhang, T. and Mao, S. (2020). Smart power control for quality-driven multi-user video transmissions: A deep reinforcement learning approach. *IEEE Access*, 8, pp. 611–622. doi: 10.1109/ACCESS.2019.2961914.